

(1) Comments from referee

The paper deals with the problem of whistler mode waves excitation by a monochromatic current placed at a certain level in the lower ionosphere. The authors aim at calculating the electromagnetic field on the ground and at a certain level above the source region, using the full-wave approach. This problem is of undoubted interest for ANGEO.

I begin with minor remarks which arise when reading the manuscript.

1. *When presenting the density profile and the profile of collision frequency, the authors refer to IRI model. As far as I know, IRI model does not provide collision frequency, at least, the URL given in the text does not lead to a site from which the collision frequency can be inferred. Thus, the given reference appears to be misleading.*
2. *Figure labels are too small and hardly readable.*
3. *Formular on page 5, line 20 is cut.*
4. *The sentence on page 8, line 4, starting with "Since a wave ..." seems to be incomplete, or the dot should be replaced by a comma.*
5. *Page 9, line 6. Poynting vector has incorrect dimension.*
6. *In the Discussion and Conclusions, which follow one after another, there are almost word-for-word repetitions.*
7. *Although the presentation is clear, there are some mistakes in English usage. For example, p.1, line 11, "by a now" should be changed to "by now". In the Acknowledgements, "was performed" should be replaced by "were performed".*
8. *However, a serious point consists in the following. The authors claim that they solve the problem under conditions that "The source current is located in the horizontal plane and can have arbitrary distribution over horizontal coordinates". This claim is then repeated in Discussion. However, the authors only explain in detail how they find the field harmonics, stating that "The coordinate dependence of the wave field can be found from the inverse Fourier transform (10)" - is it that easy? It is impossible to find numerically the Fourier transform for all n_{\perp} , thus formular (10), to which the authors refer, being suitable for analytical calculations, does not make much sense in the case of numerical ones. This point, which is*

commented in the text by one sentence, even few times ("Inverse Fourier transform yields space dependence of the wave field") needs a detailed explanation. How, using (10), have the authors found the field in coordinate presentation from inevitably discrete and finite number of Fourier transforms?

(2) Author's response

We would like to thank the Reviewer for the time he/she spent reading, positive response, and commenting our manuscript. We have prepared a point-by-point answer to his/her comments below. The responses are marked in bold.

Reviewer's Comments:

1. *When presenting the density profile of collision frequency, the authors refer to IRI model. As far as I know, IRI model does not provide collision frequency, at least, URL given in the text does not lead to a site from which the collision frequency can be inferred. Thus, the given reference appears to be misleading.*

Response:

Some clarifications concerning the collision frequency data and corresponding reference to the book of Gurevich and Shvarcburg (1973) were added to the text of the manuscript.

Reviewer's Comments:

2. *Figure labels are too small and hardly readable.*

Response:

Figure labels are enlarged.

Reviewer's Comments:

3. *Formular on page 5, line 20 is cut*

Response:

The formular was corrected.

4. *The sentence on page 8, line 4, starting with “Since a wave...” seems to be incomplete, or the dot should be replaced by a comma.*

Response:

This misprint was corrected.

Reviewer's Comments:

5. *Page 9, line 6. Poynting vector has incorrect dimension.*

Response:

This misprint was corrected.

Reviewer's Comments:

6. *In the Discussion and Conclusions, which follow one after another, there are almost word-for-word repetitions.*

Response:

The manuscript was edited.

Reviewer's Comments:

7. *Although the presentation is clear, there are some mistakes in English usage. For example, p. 1, line 11, “by a now” should be changed “by now”. In the Acknowledgements, “was performed” should be replaced by “were performed”.*

Response:

These misprints were corrected.

Reviewer's Comments:

8. *However, a serious point consist in the following. The authors claim that they solve the problem under conditions that “The source current is located in the horizontal plane and can have arbitrary distribution over horizontal coordinates”. This claim is then repeated*

in Discussions. However, the authors only explain in detail how they find the field harmonics, starting that “The coordinate dependence of the wave field can be found from the inverse Fourier transform for all n_{\perp} , thus formula(10), to which the authors refer, being suitable for analytical calculations, does not make much sense in the case of numerical ones. This point, which is commented in the text by one sentence, even few times (“Inverse Fourier transform yields space dependence of the wave field”) needs a detailed explanation. How, using (10), have the authors found the field in coordinate presentation from inevitably discrete and finite number of Fourier transforms

Response:

We used Matlab' FFT (Fast Fourier Transform) solver. Corresponding clarification and reference were added to the text of the manuscript.

(3) Author's changes in manuscript

The modified parts are marked in yellow and the removed parts are marked in red in the new marked version of the manuscript.

Whistler waves produced by monochromatic currents in the low nighttime ionosphere

Vera G. Mizonova^{1,2} and Peter A. Bespalov³

¹Nyzhny Novgorod State Technical University, Nyzhny Novgorod, Russia

²National Research University Higher School of Economics, Russia

³Institute of Applied Physics RAS, Nizhny Novgorod, Russia

Correspondence: Peter A. Bespalov

(PBespalov@mail.ru)

Abstract. We use a full-wave approach to find the field of monochromatic whistler waves, which are excited and propagating in the low nighttime ionosphere. The source current is located in the horizontal plane and can have arbitrary **finite** distribution over horizontal coordinates. The ground-based horizontal magnetic field and electric field at 125 km are calculated. The character of wave polarization on the ground surface is investigated. The percentages of source energy supplied to the Earth-ionosphere

5 waveguide and carried upward ionosphere are estimated. Received results are important for the analysis of ELF/VLF emission phenomena observed both on the satellites and on the ground.

1 Introduction

ELF/VLF waves, which propagate in the ionosphere in whistler mode, are an important part of the ionosphere dynamics. Such waves can be emitted by various natural phenomena such as atmospheric lightning discharges and volcanic eruptions, 10 magnetospheric chorus and hiss. Artificial ELF/VLF waves have been produced by ground based transmitters and by modulated HF heating of the ionosphere current system responsible for S_q variations or auroral electrojet, which is by ~~a~~ now well-known technique.

Several numerical methods have been developed for calculating of whistler wave fields in the Earth's ionosphere (Pitteway, 1965; Wait, 1970; Bossy, 1979; Nygård, 1982; Budden, 1985; Nagano et al., 1994, Yagitani et al., 1994; Shalashov and 15 Gospodchikov, 2011). One of the main difficulties is numerical instabilities caused by a large imaginary part of the vertical wave number. General full-wave analysis, including the problem of numerical 'swamping' of the evanescent wave solutions, was made, for example, by Nygård (1982), Nagano et al. (1994), Budden (1985). Full wave calculation of ELF/VLF propagation from a dipole source located in the lower ionosphere has been made by Yagitani et al. (1994). The idea of recursive calculation of mode amplitudes was developed and used for an arbitrary configuration of the radiating sources by Lehtinen and Inan (2008). 20 Nevertheless, finding fields created by both natural and artificial ELF/VLF radiating sources is still very actual.

In this paper, we use numerical methods to find the field of a whistler wave generated and propagating in low night ionosphere. We use a technique known as the two-point boundary-value problem for ordinary differential equations (Kierzenka and Shampine, 2001). Using this technique in early work (Bespalov and Mizonova, 2017; Bespalov et al., 2018) has provided

numerically stable solutions of a complete system of wave equations for arbitrary altitude profiles of plasma parameters and for arbitrary angles of wave incidence. Here, we find a wave field created by a monochromatic source current located in the low night ionosphere. As an example of calculations we use current distributions similar to those simulated by HF heating of the auroral electrojet (Payne et al., 2007). The obtained results are important for analysis of the ELF/VLF emission phenomena
5 observed both in the ground-based observatories and on board of satellites.

2 Basic equations

We consider a whistler wave which is excited and propagating in the layer $0 \leq z \leq z_{\max}$ of the non-homogeneous stratified ionosphere. We choose a coordinate system with vertical upward z axis and x, y axes in horizontal plane, suppose that plasma parameters depend on coordinate z , plane $z = 0$ corresponds to the ground surface, above the boundary $z = z_{\max}$ ionosphere
10 plasma is close to homogeneous, the ambient magnetic field \mathbf{B}_0 belongs to the y, z plane and is inclined at an angle ϑ to the z axis. We assume that external currents have monochromatic dependence on time and flow in the source plane $z = z_s$

$$\mathbf{j}(\mathbf{r}_\perp, z, t) = \mathbf{J}(\mathbf{r}_\perp) \delta(z - z_s) e^{-i\omega t}. \quad (1)$$

At first, we use the Fourier composition of the source current density over the horizontal coordinates

$$\mathbf{J}(\mathbf{n}_\perp, z) = \int \mathbf{J}(\mathbf{r}_\perp, z) e^{-ik_0 \mathbf{n}_\perp \cdot \mathbf{r}_\perp} k_0^2 d\mathbf{r}_\perp, \quad (2)$$

and wave electric and magnetic fields at each altitude

$$\begin{aligned} \mathbf{E}(\mathbf{n}_\perp, z) &= \int \mathbf{E}(\mathbf{r}_\perp, z) e^{-ik_0 \mathbf{n}_\perp \cdot \mathbf{r}_\perp} k_0^2 d\mathbf{r}_\perp, \\ \mathbf{H}(\mathbf{n}_\perp, z) &= \int \mathbf{H}(\mathbf{r}_\perp, z) e^{-ik_0 \mathbf{n}_\perp \cdot \mathbf{r}_\perp} k_0^2 d\mathbf{r}_\perp, \end{aligned} \quad (3)$$

and find field amplitudes $\mathbf{E}(\mathbf{n}_\perp, z), \mathbf{H}(\mathbf{n}_\perp, z)$ corresponding to the horizontal wave vector component $\mathbf{k}_\perp = k_0 \mathbf{n}_\perp, k_0 = \omega/c$.
15 Here we use SI units for \mathbf{E} and modified units for $\mathbf{H} = Z_0 \mathbf{H}_{SI}$ (Budden, 1985), where $Z_0 = \sqrt{\mu_0/\epsilon_0}$ is the impedance of free space. Then we write the Maxwell equations

$$\begin{aligned} \nabla \times \mathbf{H} &= Z_0 \mathbf{j} - ik_0 \hat{\epsilon} \mathbf{E}, \\ \nabla \times \mathbf{E} &= ik_0 \mathbf{H}, \end{aligned} \quad (4)$$

where c is the speed of light in free space and $\hat{\epsilon}$ is permittivity tensor, which yield a set of four equations for the horizontal components $\mathbf{E}_\perp(\mathbf{n}_\perp, z), \mathbf{H}_\perp(\mathbf{n}_\perp, z)$ (in a case of source-free medium see, e.g., Budden, 1985; Bespalov et al., 2018; Mizonova, 2019)

$$d\mathbf{F}/dz = \hat{\mathbf{M}}\mathbf{F} + Z_0 \mathbf{I} \delta(z - z_s). \quad (5)$$

Here we have taken into attention that the horizontal refractive index of the wave propagating through the stratified medium is conserved due to Snell's law. In Eq. (5) $\mathbf{F}(\mathbf{n}_\perp, z)$ and $\mathbf{I}(\mathbf{n}_\perp, z)$ are four-component column vectors

$$\mathbf{F} = \begin{pmatrix} E_x \\ E_y \\ H_x \\ H_y \end{pmatrix}, \mathbf{I} = \begin{pmatrix} n_x J_z / \varepsilon_{zz} \\ n_y J_z / \varepsilon_{zz} \\ J_y - J_z (\eta - \varepsilon) \sin 2\vartheta / 2\varepsilon_{zz} \\ -J_x + J_z i g \sin \vartheta / \varepsilon_{zz} \end{pmatrix}, \quad (6)$$

$\hat{\mathbf{M}}$ is a matrix of which the elements m_{ij} are expressed in terms of components of the transverse wave vector $\mathbf{k}_\perp = k_0 \mathbf{n}_\perp$, ε , η , g are elements of the permittivity tensor which depends on the z coordinate (Bespalov and Mizonova, 2017, Bespalov et al., 2018), $\varepsilon_{zz} = \varepsilon \sin^2 \vartheta + \eta \cos^2 \vartheta$.

To solve the system (5), (6) we define four boundary conditions. We write two of them on the plane $z = 0$ assuming the ground surface to be perfect conductive

$$E_x(z = 0) = 0, \quad E_y(z = 0) = 0. \quad (7)$$

We write two other conditions on the plane $z = z_{\max}$ excluding wave energy coming from above. To clarify them we express the field vector column F above the boundary $z = z_{\max}$ as sum of four wave modes

$$\mathbf{F}(z) = \sum_{j=1}^4 A_j \mathbf{P}_j \exp(i k_{zj} (z - z_{\max})). \quad (8)$$

10 Here $A_j = \text{const}$, k_{zj} are four roots of local dispersion relation and \mathbf{P}_j are four corresponding local polarization vectors. We mention that values k_{zj} and vectors \mathbf{P}_j are the solution of Eqs. (5), (8) for homogeneous plasma without sources. Assuming that indices 2 and 4 correspond to coming from above propagating and non-propagating wave modes (imaginary parts of k_{z2} and k_{z4} are negative) we write

$$A_2 = 0, \quad A_4 = 0. \quad (9)$$

Solving the set of Eq. (5) with known source current density (6) and boundary conditions (7), (9) we can find the field of plane 15 wave with horizontal wave vector $\mathbf{k}_\perp = k_0 \mathbf{n}_\perp$ in the layer $0 < z < z_{\max}$. Then, we use the inverse transform

$$\begin{aligned} \mathbf{E}(\mathbf{r}_\perp, z) &= \int \mathbf{E}(\mathbf{n}_\perp, z) e^{i k_0 \mathbf{n}_\perp \mathbf{r}_\perp} \frac{d\mathbf{n}_\perp}{(2\pi)^2}, \\ \mathbf{H}(\mathbf{r}_\perp, z) &= \int \mathbf{H}(\mathbf{n}_\perp, z) e^{i k_0 \mathbf{n}_\perp \mathbf{r}_\perp} \frac{d\mathbf{n}_\perp}{(2\pi)^2}, \end{aligned} \quad (10)$$

to calculate the total field.

3 Description of the solution algorithm

We take into account that out of the plane $z = z_s$ the source current density (6) is equal to zero, so Eq. (5) becomes

$$d\mathbf{F}/dz = \hat{\mathbf{M}}\mathbf{F} . \quad (11)$$

To solve Eq. (11) in layers $0 \leq z < z_s$ and $z_s < z \leq z_{\max}$ we apply packaged solver Matlab's bvp4c and use a method of known as the two-point boundary-value problem for ordinary differential equations (Kierzenka and Shampine, 2001). The 5 solver solution starts with an initial guess supplied at an initial mesh points and changes step-size to get the specified accuracy.

At first we find two linearly independent solutions \mathbf{F}_1 and \mathbf{F}_2 of Eq. (11) in the layer $0 \leq z < z_s$ completing the boundary condition (7) on the plane $z = 0$ for arbitrary conditions on the plane $z = z_s - 0$. For example, we use four conditions $E_x(z = 0) = 0, E_y(z = 0) = 0, E_x(z = z_s - 0) = \mathfrak{E}, E_y(z = z_s - 0) = 0$ for the solution \mathbf{F}_1 and four conditions $E_x(z = 0) = 0, E_y(z = 0) = 0, E_x(z = z_s - 0) = 0, E_y(z = z_s - 0) = \mathfrak{E}$ for the solution \mathbf{F}_2 , where \mathfrak{E} is constant. Then we write the general solution in the layer $0 \leq z \leq z_s$ as sum

$$\mathbf{F} = a\mathbf{F}_1 + b\mathbf{F}_2 . \quad (12)$$

Similarly, we find two linearly independent solutions \mathbf{F}_1^* and \mathbf{F}_2^* of Eq. (11) in the upper layer $z_s < z \leq z_{\max}$ completing the boundary condition (9) on the plane $z = z_{\max}$. By arbitrary conditions on the plane $z = z_s + 0$ we have $A_2 = 0, A_4 = 0, E_x(z = z_s + 0) = \mathfrak{E}, E_y(z = z_s + 0) = 0$ and $A_2 = 0, A_4 = 0, E_x(z = z_s + 0) = 0, E_y(z = z_s + 0) = \mathfrak{E}$ respectively. We write the general solution in the layer $z_s < z \leq z_{\max}$ as sum

$$\mathbf{F} = a^*\mathbf{F}_1^* + b^*\mathbf{F}_2^* . \quad (13)$$

15 Integrating Eq. (5) over z coordinate in a narrow layer $(z_s - 0, z_s + 0)$ we find a condition connecting solutions (12) and (13)

$$\mathbf{F}(z = z_s + 0) - \mathbf{F}(z = z_s - 0) = Z_0\mathbf{I} . \quad (14)$$

That condition yields four algebraic equations for the coefficients a, a^*, b, b^* . Thus, finding those coefficients we obtain the wave field F (6) in the layer $0 \leq z \leq z_{\max}$. In particular, the fields on the ground surface can be expressed as

$$\begin{aligned} H_{\perp}(z = 0) &= \sqrt{|H_x(z = 0)|^2 + |H_y(z = 0)|^2}, \\ E_{y'}(z = 0) &= \left(\sin \vartheta - \frac{n_y}{n_{0z}} \cos \vartheta \right) n_x H_y(z = 0) - \\ &\quad - \left((1 - n_y^2) \frac{\cos \vartheta}{n_{0z}} + n_y \sin \vartheta \right) H_x(z = 0), \\ E_{x'}(z = 0) &= \frac{1 - n_x^2}{n_{0z}} H_y(z = 0) + \frac{n_x n_y}{n_{0z}} H_x(z = 0), \end{aligned} \quad (15)$$

where $n_{0z} = \sqrt{1 - n_{\perp}^2}$, $E_{x',y'}$ are electric strength components of incident wave in coordinate system with z' - axis along ambient magnetic field. The wave polarization near the ground surface is determined by

$$\Pi = E_{y'}(z = 0) / E_{x'}(z = 0) . \quad (16)$$

The electric field at the altitude $z = z_{\max}$ can be expressed as

$$\begin{aligned} E(z = z_{\max}) &= \\ &= \sqrt{|E_x(z = z_{\max})|^2 + |E_y(z = z_{\max})|^2 + |E_z(z = z_{\max})|^2} . \end{aligned} \quad (17)$$

The coordinate dependence of the wave field can be found from the inverse Fourier transform (10). The vertical energy flux

5 (Poynting vector) is

$$S_z = (2Z_0)^{-1} \operatorname{Re} [\mathbf{E}_{\perp}^* \cdot \mathbf{H}_{\perp}]_z , \quad (18)$$

and the total power of source is

$$P = \frac{1}{2} \operatorname{Re} \int (j_x E_x^*(z = z_s) + j_y E_y^*(z = z_s)) dx dy . \quad (19)$$

Now we present the results of numerically computed solution of the set (5), (6) under model conditions for the nighttime ionosphere.

4 The ionosphere data and calculation results

10 In the calculations, we use the altitude profiles of the plasma density shown in Fig. 1a, and the collision frequencies between charged and neutral particles shown in Fig. 1b. The **plasma density** data are taken from International Reference Ionosphere (Bilitza and Reinisch, 2007) (https://ccmc.gsfc.nasa.gov/modelweb/models/iri2016_vitmo.php) and correspond to 68° N; 25° E; 04 September 2019, 00:30 LT. **The collision frequencies data are taken from the book of Gurevich and Shvarcburg (1973).** The angle of magnetic field inclination with respect to the axis z is equal to $\vartheta = 168^0$. We use the value

15 $z_{\max} = 125$ km as the upper boundary of the solution. At this altitude a typical scale of plasma inhomogeneity exceeds 70 km and is much more than the wavelength which in the considered case is of order from 20 to 25 km. As an example, we calculate the fields created by varying at frequency 3 kHz and flowing at the altitude $z_s = 80$ km horizontal current, with equal x and y components $J_x = J_y$ and $J_z = 0$. We assume that currents occupy a volume which has a shape of a horizontal pancake and use for calculations a Gaussian distributions over x and y coordinates $J(\mathbf{r}_{\perp}) = J_{\max} \exp(-x^2/2L_x^2 - y^2/2L_y^2)$ with characteristic horizontal sizes $L_x = 12$ km, $L_y = 70$ km. Corresponding current distribution (2) in Fourier-space is also Gaussian and has a form $J(\mathbf{n}_{\perp}) = J_0 \exp(-k_x^2 L_x^2 n_x^2/2 - k_y^2 L_y^2 n_y^2/2)$, where $J_0 = 2\pi k_0^2 L_x L_y J_{\max}$. **We calculate the wave field in $N = 400$ points with steps and then use inverse Fast Fourier transform (Cooley and Tukey, 1965) to find its coordinate dependence.** We present the results of field calculation in Fourier-space (Figs. 2-3) and in coordinate space (Fig. 4).

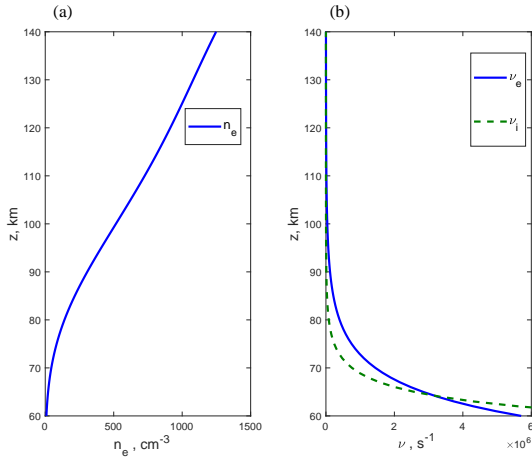


Figure 1. Nighttime ionosphere model: (a) the electron plasma density and (b) the collision frequency between electron and neutral particles (solid line) and collision frequency between ion and neutral particles (dashed line).

The dependences of amplitude of horizontal magnetic field $H_{\perp}(n_x, n_y)/E_0$ on ground surface $z = 0$ and amplitude of electric field $E(n_x, n_y)/E_0$ at altitude $z = z_{\max}$ are presented in Figs. 2a,b. The field values are normalized by the value $E_0 = Z_0 J_0$. Polarization ellipse parameters ϕ , $E_{y'} = E_{x'} e^{-i\phi}$ and $\log|E_{y'}/E_{x'}|$ are presented in Figs. 2c,d. Positive values of phase ϕ correspond to right hand polarization, typical for whistler waves, and negative values of phase ϕ correspond to left hand polarization. Positive values of parameter $\log|E_{y'}/E_{x'}|$ mean that the polarization ellipse is elongated predominantly along y axis and negative values of parameter $\log|E_{y'}/E_{x'}|$ mean that the polarization ellipse is elongated predominantly along x axis. Examples of altitude dependences of normalized electric and magnetic fields corresponding to different horizontal wave vectors are presented in Fig. 3. The level $z = z_s$ of source action is marked by dotted line. Figures 4 shows contour maps of fields created by horizontal currents with known space distribution. Figure 4a shows current density normalized by the value J_{\max} . Figure 4b shows electric field at the altitude $z = z_{\max}$. Figure 4c shows horizontal magnetic field on ground surface $z = 0$. Both electric and magnetic fields are normalized by the value $Z_0 J_{\max}$. Figure 4d shows polarization parameter ϕ . The arrow shows the current direction.

5 Discussion

We use a full-wave approach to find the field of monochromatic whistler waves which are excited and propagating at night in the strongly inhomogeneous low ionosphere. A source current is assumed to be located in horizontal plane and to have in this plane an arbitrary **finite** space distribution. At first, we consider a plane wave with the horizontal components of the refractive index \mathbf{n}_{\perp} generated by the current $J(\mathbf{r}_{\perp}) \sim e^{ik_0 \mathbf{n}_{\perp} \cdot \mathbf{r}_{\perp}}$. The set of wave equation in the layer $0 < z < z_{\max}$ for each \mathbf{n}_{\perp} - component is completed by boundary conditions assuming a perfect conductivity of ground surface and excluding wave

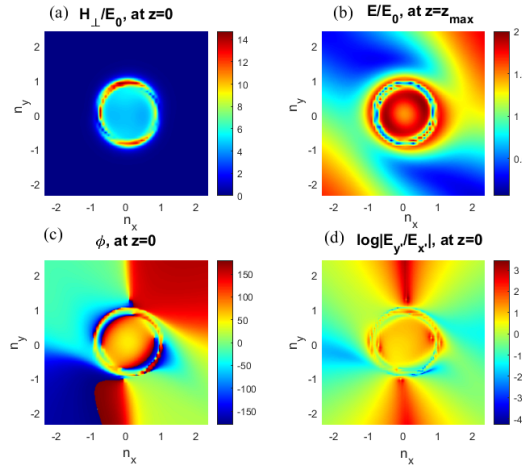


Figure 2. Fields in the $z = 0$ plane: (a) the horizontal magnetic field, (b) the electric field at the height $z = 125$ km, (c) the polarization ellipse parameters ϕ ($E_{y'} = E_{x'} e^{i\phi}$), and (d) $\log|E_{y'}/E_{x'}|$.

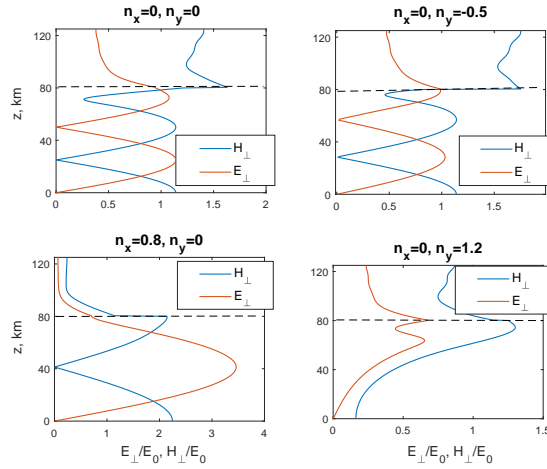


Figure 3. Altitude dependences of the amplitudes of horizontal electric and magnetic fields.

energy coming on the upper boundary $z = z_{\max}$ from above. The method known as the two-point boundary-value problem for ordinary differential equations (Kierzenka and Shampine, 2001) is applied to find the solutions of wave equations above and below the source plane. Then we connect these solutions using source current distribution. **When the dependencies of source current and wave field in n_{\perp} -space are finite functions with discretized values, the Fast Fourier Transform algorithm can be used for numerical calculations.** Inverse Fast Fourier transform yields space dependence of the wave field.

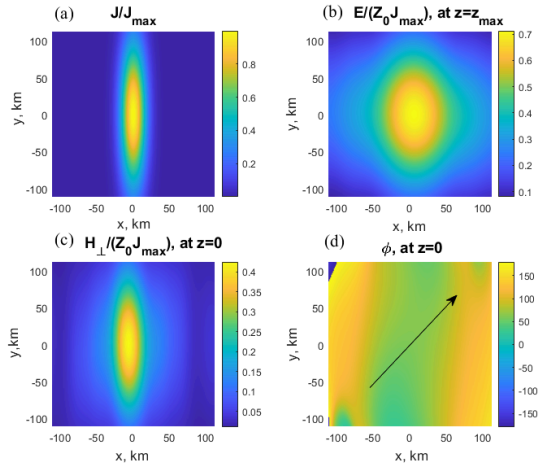


Figure 4. Source currents and fields space distributions: (a) space distributions of source currents, (b) the electric field at $z = 125$ km, (c) the horizontal magnetic field at $z = 0$, and (d) the polarization ellipse parameters ϕ , $E_{y'} = E_{x'} e^{-i\phi}$ at $z = 0$.

As an example, we calculate the fields created by varying at a frequency of 3 kHz and flowing at $z_s = 80$ km horizontal current, with coincided x and y components of current density $J_x = J_y$. We use a Gaussian distributions of source current density over x and y coordinates with characteristic horizontal sizes $L_x = 12$ km, $L_y = 70$ km. We mention that the model of a plane source current can also be effective in a more general case of current layer with small thickness $\Delta z \ll \lambda_z \sim 60$ km.

5 The ground-based horizontal magnetic field and the electric field at 125 km are calculated both in Fourier (n_x , n_y) and coordinate (x , y) spaces. Since a wave can achieve the ground surface in penetrating mode in case $n_{\perp} \leq 1$. The magnetic field $H_{\perp}(\mathbf{n}_{\perp}, z = 0)$ is noticeably non-zero for Fourier components with $n_{\perp} < 1$ and is practically equal to zero for Fourier components with $n_{\perp} \gg 1$. Waves with $n_{\perp} < 1$ are right hand polarized (see Fig. 2c), which is typical for whistlers. However, if the horizontal component of the refractive index has an order of unit, then the magnetic field $H_{\perp}(\mathbf{n}_{\perp}, z = 0)$ can increase 10 two or three times (see Fig. 2a). The polarization parameter ϕ of such components can be negative similar to the left hand polarized waves (see Fig. 2c). We mention that if the horizontal size of radiating currents is small enough $L \leq 1/k_0 \sim 15$ km (for wave with frequency 3 kHz) then Fourier components with $n_{\perp} \sim 1$ can make a noticeable contribution into the whole field and change the character of polarization.

15 The magnetic field $H_{\perp}(\mathbf{r}_{\perp}, z = 0)$ is predominantly localized under the source (Fig. 4c). The electric field at 125 km occupies a spot of several times larger size (Fig. 4b). The polarization parameter ϕ at $z = 0$ is positive almost everywhere, but becomes negative at large distances from the source across the current direction (Fig. 4d). We mention that the used in our calculation current distributions can be similar to electrojet currents modulated in D-region by the HAARP HF heating facility (Keskinen and Rowland, 2006; Payne et al., 2007). For example, according to data collected during an experimental campaign run in April 2003 and results of numerical simulations (Payne et al., 2007; Lehtinen and Inan, 2008), the maximum change in

modulated conductivity occupies approximately 10 km over the height and occurs at altitude ~ 80 km. Pedersen and Hall conductivities approximately coincide so if ambient electrojet field is directed along x axis, then $j_x \approx j_y$. The maximum surface density of modulated currents has an order $J_{\max} \sim 10^{-6} \div 10^{-5} \text{ Am}^{-1}$. Using in our calculations the magnitude of current density $J_{\max} \sim 5 \cdot 10^{-6} \text{ Am}^{-1}$ yields the total power of the source $\sim 36 \text{ W}$, the ground-based horizontal magnetic field under the source $B_{\perp} \sim 1 \text{ pT}$ and the electric field at the altitude of 125 km above the source $E \sim 400 \mu \text{Vm}^{-1}$. The magnitude of the magnetic field is similar to the field measured at VLF sites in the immediate vicinity of the HAARP heating facility (Payne et al., 2007) and calculated by Lehtinen and Inan (2008). The maximum vertical energy flux (Poynting vector) at the altitude of 125 km is $\sim 3,2 \text{nWm}^{-1}$ and total power is $\sim 17 \text{ W}$. The percentages of source energy supplied by the Earth-ionosphere waveguide and carried upward ionosphere depends on altitude profile of ionosphere plasma. If low boundary of ionosphere is sharp enough then sufficient part of the source energy is supplied to the Earth-ionosphere waveguide. In a case of smooth ionosphere low boundary sufficient part of the source energy is carried upward. By used for calculation altitude profile of plasma density about half of the source energy is carried upward, approximately twenty percent of the energy is supplied to the Earth-ionosphere waveguide and approximately thirty percent of the energy is absorbed.

6 Conclusions

We find a field of monochromatic whistler waves which are excited and propagating in the low nighttime ionosphere. ~~Using a technique known as the two point boundary value problem for ordinary differential equations~~ **Using a MatLab boundary-value problem solver** enables to find numerically stable solutions of full set of the wave equations applying to conditions of inhomogeneous ionosphere at altitudes below 125 km. Above this altitude the ionosphere plasma is slightly inhomogeneous, hence approximate methods are suitable. As example, this calculation technique is applied to the problem of ELF/VLF waves radiation from modulated HF-heated electrojet currents. At first we consider a plane wave with known horizontal component of the refractive index, find a wave field and analyze a character of wave polarization on the ground surface. Then we use **inverse Fourier transform** to find a total field, **get the dependencies of wave field at 0 km and 125 km, analyze the type of wave polarization on the ground surface and estimate absorbed, supplied by the earth-ionosphere waveguide and carried upward parts of source energy**. ~~The ground-based magnetic field is predominantly located under the source. The wave field at 125 km occupies a spot of several times larger size. The polarization almost everywhere is typical for whistlers (right hand), but at large distances from the source across the current direction can become left hand. About half of the source energy is carried upward, approximately twenty percent of the energy is supplied to the Earth-ionosphere waveguide and approximately thirty percent of the energy is absorbed.~~ The obtained values are in a good agreement with ground and satellite observations and known calculation results. Using model of plane horizontal source currents can be generalized for the arbitrary altitude source distribution.

Data availability. The paper is theoretical and no new experimental data are used. The data are taken from International Reference Ionosphere model (Bilitza and Reinisch, 2007) (https://ccmc.gsfc.nasa.gov/modelweb/models/iri2016_vitmo.php). All figures are obtained from numerical calculation in MATLAB codes.

Author contributions. VM produced the calculations, analyzed results, and wrote the paper. PB proposed the problem, discussed results, and wrote the paper.

Competing interests. The authors declare that they have no conflict of interest.

Acknowledgements. The work (Sections 2-4) is supported by RFBR grant No. 20-02-00206A. The work of P.A. Bespalov (Sections 1, 5, and 6) is supported by RSF grant No. 20-12-00268. The numerical calculations were performed as part of the State Assignment of the Institute of Applied Physics RAS, project No.0035-2019-0002.

References

Bespalov, P. and Mizonova, V.: Propagation of a whistler wave incident from above on the lower nighttime ionosphere, *Ann. Geophys.*, 35, 671-675, <http://dx.doi.org/10.5194/angeo-35-671-2017>, 2017.

Bespalov, P.A., Mizonova V.G., and Savina, O.N.: Reflection from and transmission through the ionosphere of VLF electromagnetic waves incident from the mid-latitude magnetosphere, *J. Atmos. Sol.-Terr. Phys.*, 175, 40-48, <https://doi.org/10.1016/j.jastp.2018.04.018>, 2018.

Bilitza, D., and Reinisch, B.: International reference ionosphere: improvements and new parameters, *J. Adv. Space Res.*, 42, 599 - 609, <http://dx.doi.org/10.1029/2007SW000359>, 2007.

Bossy, L.: Wave propagation in stratified anisotropic media, *J. Geophys.*, 46, 1-14, 1979.

Budden, K.G.: The propagation of radio waves: the theory of radio waves of low power in the ionosphere and magnetosphere, Cambridge Univ. Press, Cambridge, 1985.

Cooley, W. and Tukey, J.W.I.: An algorithm for the machine calculation of complex Fourier series, *Math. Comp.*, 19, 297-301, <https://doi.org/10.1090/S0025-5718-1965-0178586-1>, 1965.

Gurevich, A.V. and Shvareburg, A.B.: Nonlinear theory of radio wave propagation in the ionosphere, Nauka, Moscow, 1973 [in Russian].

Keskinen, M.J., and Rowland, H.L.: Magnetospheric effects from man-made ELF/VLF modulation of the auroral electrojet, *Radio Sci.*, 41, RS1006, <https://doi:10.1029/2005RS003274>, 2006.

Kierzenka, J., and Shampine, L.F.: A BVP Solver based on Residual Control and the MATLAB PSE , *ACM TOMS.*, 27, 3, 299-316, 2001.

Lehtinen, N.G., and Inan, U.S.: Radiation of ELF/VLF waves by harmonically varying currents into a stratified ionosphere with application to radiation by a modulated electrojet, *J. Geophys. Res.*, 113, A06301. <http://dx.doi.org/10.1029/2007JA012911>, 2008.

Mizonova, V.G.: Matrix Algorithm of Approximate Solution of Wave Equations in Inhomogeneous Magnetoactive Plasma, *Plasma Phys. Rep.*, 45, 8, 777-785, <https://doi:10.1134/S1063780X190700802019>, 2019.

Nagano, I., Miyamura, K., Yagitani, S., Kimura, I., Okada, T., Hashimoto, K., and Wong, A.Y.: Full wave calculation method of VLF wave radiated from a dipole antenna in the ionosphere - analysis of joint experiment by HIPAS and Akebono satellite, *Electr. Commun. Jpn. Commun.*, 77, 59-71, <http://dx.doi.org/10.1002/ecja.4410771106>, 1994.

Nygre'n, T.: A method of full wave analysis with improved stability, *Planet. Space Sci.*, 30(4), 427-430, [http://dx.doi.org/10.1016/0032-0633\(82\)90048-4](http://dx.doi.org/10.1016/0032-0633(82)90048-4), 1982.

Payne, J.A., Inan, U.S., Foust, F.R., Chevalier, T.W., and Bell, T.F.: HF modulated ionospheric currents, *Geophys. Res. Lett.*, 34, L23101, <http://doi:10.1029/2007GL031724>, 2007.

Pitteway, M.L.V.: The numerical calculation of wave-fields, reflection coefficients and polarizations for long radio waves in the lower ionosphere, *I. Phil. Trans. R. Soc. London, Ser. A*, 257(1079), 219-241, 1965.

Shalashov, A. G. and Gospodchikov, E. D.: Impedance technique for modeling electromagnetic wave propagation in anisotropic and gyroscopic media, *Physics-Uspekhi*, 54, 145- 165, <https://doi.org/10.3367/UFNe.0181.201102c.0151>, 2011.

Wait, J.R.: Electromagnetic waves in stratified media, 2nd ed., Pergamon, New York, 1970.

Yagitani, S., Nagano, I., Miyamura, K., and Kimura, I.: Full wave calculation of ELF/VLF propagation from a dipole source located in the lower ionosphere, *Radio Sci.*, 29, 39-54, <https://doi:10.1029/93RS01728>, 1994.

Whistler waves produced by monochromatic currents in the low nighttime ionosphere

Vera G. Mizonova^{1,2} and Peter A. Bespalov³

¹Nyzhny Novgorod State Technical University, Nyzhny Novgorod, Russia

²National Research University Higher School of Economics, Russia

³Institute of Applied Physics RAS, Nizhny Novgorod, Russia

Correspondence: Peter A. Bespalov

(PBespalov@mail.ru)

Abstract. We use a full-wave approach to find the field of monochromatic whistler waves, which are excited and propagating in the low nighttime ionosphere. The source current is located in the horizontal plane and can have arbitrary **finite** distribution over horizontal coordinates. The ground-based horizontal magnetic field and electric field at 125 km are calculated. The character of wave polarization on the ground surface is investigated. The percentages of source energy supplied to the Earth-ionosphere waveguide and carried upward ionosphere are estimated. Received results are important for the analysis of ELF/VLF emission phenomena observed both on the satellites and on the ground.

1 Introduction

ELF/VLF waves, which propagate in the ionosphere in whistler mode, are an important part of the ionosphere dynamics. Such waves can be emitted by various natural phenomena such as atmospheric lightning discharges and volcanic eruptions, 10 magnetospheric chorus and hiss. Artificial ELF/VLF waves have been produced by ground based transmitters and by modulated HF heating of the ionosphere current system responsible for S_q variations or auroral electrojet, which is by now well-known technique.

Several numerical methods have been developed for calculating of whistler wave fields in the Earth's ionosphere (Pitteway, 1965; Wait, 1970; Bossy, 1979; Nygård, 1982; Budden, 1985; Nagano et al., 1994, Yagitani et al., 1994; Shalashov and 15 Gospodchikov, 2011). One of the main difficulties is numerical instabilities caused by a large imaginary part of the vertical wave number. General full-wave analysis, including the problem of numerical 'swamping' of the evanescent wave solutions, was made, for example, by Nygård (1982), Nagano et al. (1994), Budden (1985). Full wave calculation of ELF/VLF propagation from a dipole source located in the lower ionosphere has been made by Yagitani et al. (1994). The idea of recursive calculation of mode amplitudes was developed and used for an arbitrary configuration of the radiating sources by Lehtinen and Inan (2008). 20 Nevertheless, finding fields created by both natural and artificial ELF/VLF radiating sources is still very actual.

In this paper, we use numerical methods to find the field of a whistler wave generated and propagating in low night ionosphere. We use a technique known as the two-point boundary-value problem for ordinary differential equations (Kierzenka and Shampine, 2001). Using this technique in early work (Bespalov and Mizonova, 2017; Bespalov et al., 2018) has provided

numerically stable solutions of a complete system of wave equations for arbitrary altitude profiles of plasma parameters and for arbitrary angles of wave incidence. Here, we find a wave field created by a monochromatic source current located in the low night ionosphere. As an example of calculations we use current distributions similar to those simulated by HF heating of the auroral electrojet (Payne et al., 2007). The obtained results are important for analysis of the ELF/VLF emission phenomena
5 observed both in the ground-based observatories and on board of satellites.

2 Basic equations

We consider a whistler wave which is excited and propagating in the layer $0 \leq z \leq z_{\max}$ of the non-homogeneous stratified ionosphere. We choose a coordinate system with vertical upward z axis and x, y axes in horizontal plane, suppose that plasma parameters depend on coordinate z , plane $z = 0$ corresponds to the ground surface, above the boundary $z = z_{\max}$ ionosphere
10 plasma is close to homogeneous, the ambient magnetic field \mathbf{B}_0 belongs to the y, z plane and is inclined at an angle ϑ to the z axis. We assume that external currents have monochromatic dependence on time and flow in the source plane $z = z_s$

$$\mathbf{j}(\mathbf{r}_\perp, z, t) = \mathbf{J}(\mathbf{r}_\perp) \delta(z - z_s) e^{-i\omega t}. \quad (1)$$

At first, we use the Fourier composition of the source current density over the horizontal coordinates

$$\mathbf{J}(\mathbf{n}_\perp, z) = \int \mathbf{J}(\mathbf{r}_\perp, z) e^{-ik_0 \mathbf{n}_\perp \cdot \mathbf{r}_\perp} k_0^2 d\mathbf{r}_\perp, \quad (2)$$

and wave electric and magnetic fields at each altitude

$$\begin{aligned} \mathbf{E}(\mathbf{n}_\perp, z) &= \int \mathbf{E}(\mathbf{r}_\perp, z) e^{-ik_0 \mathbf{n}_\perp \cdot \mathbf{r}_\perp} k_0^2 d\mathbf{r}_\perp, \\ \mathbf{H}(\mathbf{n}_\perp, z) &= \int \mathbf{H}(\mathbf{r}_\perp, z) e^{-ik_0 \mathbf{n}_\perp \cdot \mathbf{r}_\perp} k_0^2 d\mathbf{r}_\perp, \end{aligned} \quad (3)$$

and find field amplitudes $\mathbf{E}(\mathbf{n}_\perp, z), \mathbf{H}(\mathbf{n}_\perp, z)$ corresponding to the horizontal wave vector component $\mathbf{k}_\perp = k_0 \mathbf{n}_\perp, k_0 = \omega/c$.
15 Here we use SI units for \mathbf{E} and modified units for $\mathbf{H} = Z_0 \mathbf{H}_{SI}$ (Budden, 1985), where $Z_0 = \sqrt{\mu_0/\epsilon_0}$ is the impedance of free space. Then we write the Maxwell equations

$$\begin{aligned} \nabla \times \mathbf{H} &= Z_0 \mathbf{j} - ik_0 \hat{\epsilon} \mathbf{E}, \\ \nabla \times \mathbf{E} &= ik_0 \mathbf{H}, \end{aligned} \quad (4)$$

where c is the speed of light in free space and $\hat{\epsilon}$ is permittivity tensor, which yield a set of four equations for the horizontal components $\mathbf{E}_\perp(\mathbf{n}_\perp, z), \mathbf{H}_\perp(\mathbf{n}_\perp, z)$ (in a case of source-free medium see, e.g., Budden, 1985; Bespalov et al., 2018; Mizonova, 2019)

$$d\mathbf{F}/dz = \hat{\mathbf{M}}\mathbf{F} + Z_0 \mathbf{I} \delta(z - z_s). \quad (5)$$

Here we have taken into attention that the horizontal refractive index of the wave propagating through the stratified medium is conserved due to Snell's law. In Eq. (5) $\mathbf{F}(\mathbf{n}_\perp, z)$ and $\mathbf{I}(\mathbf{n}_\perp, z)$ are four-component column vectors

$$\mathbf{F} = \begin{pmatrix} E_x \\ E_y \\ H_x \\ H_y \end{pmatrix}, \mathbf{I} = \begin{pmatrix} n_x J_z / \varepsilon_{zz} \\ n_y J_z / \varepsilon_{zz} \\ J_y - J_z (\eta - \varepsilon) \sin 2\vartheta / 2\varepsilon_{zz} \\ -J_x + J_z i g \sin \vartheta / \varepsilon_{zz} \end{pmatrix}, \quad (6)$$

$\hat{\mathbf{M}}$ is a matrix of which the elements m_{ij} are expressed in terms of components of the transverse wave vector $\mathbf{k}_\perp = k_0 \mathbf{n}_\perp$, ε , η , g are elements of the permittivity tensor which depends on the z coordinate (Bespalov and Mizonova, 2017, Bespalov et al., 2018), $\varepsilon_{zz} = \varepsilon \sin^2 \vartheta + \eta \cos^2 \vartheta$.

To solve the system (5), (6) we define four boundary conditions. We write two of them on the plane $z = 0$ assuming the ground surface to be perfect conductive

$$E_x(z = 0) = 0, \quad E_y(z = 0) = 0. \quad (7)$$

We write two other conditions on the plane $z = z_{\max}$ excluding wave energy coming from above. To clarify them we express the field vector column F above the boundary $z = z_{\max}$ as sum of four wave modes

$$\mathbf{F}(z) = \sum_{j=1}^4 A_j \mathbf{P}_j \exp(i k_{zj} (z - z_{\max})). \quad (8)$$

10 Here $A_j = \text{const}$, k_{zj} are four roots of local dispersion relation and \mathbf{P}_j are four corresponding local polarization vectors. We mention that values k_{zj} and vectors \mathbf{P}_j are the solution of Eqs. (5), (8) for homogeneous plasma without sources. Assuming that indices 2 and 4 correspond to coming from above propagating and non-propagating wave modes (imaginary parts of k_{z2} and k_{z4} are negative) we write

$$A_2 = 0, \quad A_4 = 0. \quad (9)$$

Solving the set of Eq. (5) with known source current density (6) and boundary conditions (7), (9) we can find the field of plane 15 wave with horizontal wave vector $\mathbf{k}_\perp = k_0 \mathbf{n}_\perp$ in the layer $0 < z < z_{\max}$. Then, we use the inverse transform

$$\begin{aligned} \mathbf{E}(\mathbf{r}_\perp, z) &= \int \mathbf{E}(\mathbf{n}_\perp, z) e^{i k_0 \mathbf{n}_\perp \mathbf{r}_\perp} \frac{d\mathbf{n}_\perp}{(2\pi)^2}, \\ \mathbf{H}(\mathbf{r}_\perp, z) &= \int \mathbf{H}(\mathbf{n}_\perp, z) e^{i k_0 \mathbf{n}_\perp \mathbf{r}_\perp} \frac{d\mathbf{n}_\perp}{(2\pi)^2}, \end{aligned} \quad (10)$$

to calculate the total field.

3 Description of the solution algorithm

We take into account that out of the plane $z = z_s$ the source current density (6) is equal to zero, so Eq. (5) becomes

$$d\mathbf{F}/dz = \hat{\mathbf{M}}\mathbf{F} . \quad (11)$$

To solve Eq. (11) in layers $0 \leq z < z_s$ and $z_s < z \leq z_{\max}$ we apply packaged solver Matlab's bvp4c and use a method of known as the two-point boundary-value problem for ordinary differential equations (Kierzenka and Shampine, 2001). The 5 solver solution starts with an initial guess supplied at an initial mesh points and changes step-size to get the specified accuracy.

At first we find two linearly independent solutions \mathbf{F}_1 and \mathbf{F}_2 of Eq. (11) in the layer $0 \leq z < z_s$ completing the boundary condition (7) on the plane $z = 0$ for arbitrary conditions on the plane $z = z_s - 0$. For example, we use four conditions $E_x(z = 0) = 0, E_y(z = 0) = 0, E_x(z = z_s - 0) = \mathfrak{E}, E_y(z = z_s - 0) = 0$ for the solution \mathbf{F}_1 and four conditions $E_x(z = 0) = 0, E_y(z = 0) = 0, E_x(z = z_s - 0) = 0, E_y(z = z_s - 0) = \mathfrak{E}$ for the solution \mathbf{F}_2 , where \mathfrak{E} is constant. Then we write the general solution in the layer $0 \leq z \leq z_s$ as sum

$$\mathbf{F} = a\mathbf{F}_1 + b\mathbf{F}_2 . \quad (12)$$

Similarly, we find two linearly independent solutions \mathbf{F}_1^* and \mathbf{F}_2^* of Eq. (11) in the upper layer $z_s < z \leq z_{\max}$ completing the boundary condition (9) on the plane $z = z_{\max}$. By arbitrary conditions on the plane $z = z_s + 0$ we have $A_2 = 0, A_4 = 0, E_x(z = z_s + 0) = \mathfrak{E}, E_y(z = z_s + 0) = 0$ and $A_2 = 0, A_4 = 0, E_x(z = z_s + 0) = 0, E_y(z = z_s + 0) = \mathfrak{E}$ respectively. We write the general solution in the layer $z_s < z \leq z_{\max}$ as sum

$$\mathbf{F} = a^*\mathbf{F}_1^* + b^*\mathbf{F}_2^* . \quad (13)$$

15 Integrating Eq. (5) over z coordinate in a narrow layer $(z_s - 0, z_s + 0)$ we find a condition connecting solutions (12) and (13)

$$\mathbf{F}(z = z_s + 0) - \mathbf{F}(z = z_s - 0) = Z_0\mathbf{I} . \quad (14)$$

That condition yields four algebraic equations for the coefficients a, a^*, b, b^* . Thus, finding those coefficients we obtain the wave field F (6) in the layer $0 \leq z \leq z_{\max}$. In particular, the fields on the ground surface can be expressed as

$$\begin{aligned} H_{\perp}(z = 0) &= \sqrt{|H_x(z = 0)|^2 + |H_y(z = 0)|^2}, \\ E_{y'}(z = 0) &= \left(\sin \vartheta - \frac{n_y}{n_{0z}} \cos \vartheta \right) n_x H_y(z = 0) - \\ &- \left((1 - n_y^2) \frac{\cos \vartheta}{n_{0z}} + n_y \sin \vartheta \right) H_x(z = 0), \\ E_{x'}(z = 0) &= \frac{1 - n_x^2}{n_{0z}} H_y(z = 0) + \frac{n_x n_y}{n_{0z}} H_x(z = 0), \end{aligned} \quad (15)$$

where $n_{0z} = \sqrt{1 - n_{\perp}^2}$, $E_{x',y'}$ are electric strength components of incident wave in coordinate system with z' - axis along ambient magnetic field. The wave polarization near the ground surface is determined by

$$\Pi = E_{y'}(z = 0) / E_{x'}(z = 0) . \quad (16)$$

The electric field at the altitude $z = z_{\max}$ can be expressed as

$$\begin{aligned} E(z = z_{\max}) &= \\ &= \sqrt{|E_x(z = z_{\max})|^2 + |E_y(z = z_{\max})|^2 + |E_z(z = z_{\max})|^2} . \end{aligned} \quad (17)$$

The coordinate dependence of the wave field can be found from the inverse Fourier transform (10). The vertical energy flux 5 (Poynting vector) is

$$S_z = (2Z_0)^{-1} \operatorname{Re} [\mathbf{E}_{\perp}^* \cdot \mathbf{H}_{\perp}]_z , \quad (18)$$

and the total power of source is

$$P = \frac{1}{2} \operatorname{Re} \int (j_x E_x^*(z = z_s) + j_y E_y^*(z = z_s)) dx dy . \quad (19)$$

Now we present the results of numerically computed solution of the set (5), (6) under model conditions for the nighttime ionosphere.

4 The ionosphere data and calculation results

10 In the calculations, we use the altitude profiles of the plasma density shown in Fig. 1a, and the collision frequencies between charged and neutral particles shown in Fig. 1b. The plasma density data are taken from International Reference Ionosphere (Bilitzta and Reinisch, 2007) (https://ccmc.gsfc.nasa.gov/modelweb/models/iri2016_vitmo.php) and correspond to 68^0 N; 25^0 E; 04 September 2019, 00:30 LT. The collision frequencies data are taken from the book of Gurevich and Shvarcburg (1973). The angle of magnetic field inclination with respect to the axis z is equal to $\vartheta = 168^0$. We use the value $z_{\max} = 125$ km as the 15 upper boundary of the solution. At this altitude a typical scale of plasma inhomogeneity exceeds 70 km and is much more than the wavelength which in the considered case is of order from 20 to 25 km. As an example, we calculate the fields created by varying at frequency 3 kHz and flowing at the altitude $z_s = 80$ km horizontal current, with equal x and y components $J_x = J_y$ and $J_z = 0$. We assume that currents occupy a volume which has a shape of a horizontal pancake and use for calculations a Gaussian distributions over x and y coordinates $J(\mathbf{r}_{\perp}) = J_{\max} \exp(-x^2/2L_x^2 - y^2/2L_y^2)$ with characteristic horizontal sizes 20 $L_x = 12$ km, $L_y = 70$ km. Corresponding current distribution (2) in Fourier-space is also Gaussian and has a form $J(\mathbf{n}_{\perp}) = J_0 \exp(-k_x^2 L_x^2 n_x^2/2 - k_y^2 L_y^2 n_y^2/2)$, where $J_0 = 2\pi k_0^2 L_x L_y J_{\max}$. We calculate the wave field in $N = 400$ points with steps and then use inverse Fast Fourier transform (Cooley and Tukey, 1965) to find its coordinate dependence. We present the results of field calculation in Fourier-space (Figs. 2-3) and in coordinate space (Fig. 4). The dependences of amplitude of

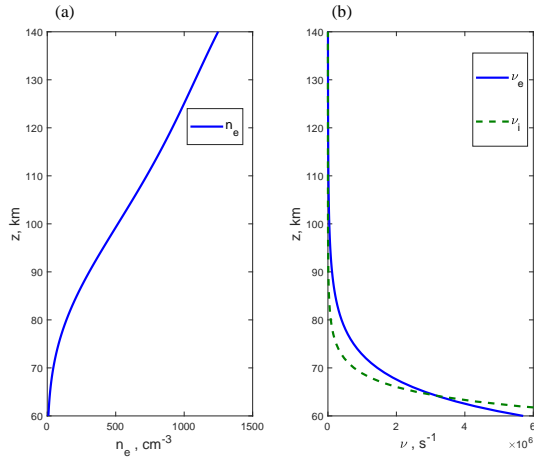


Figure 1. Nighttime ionosphere model: (a) the electron plasma density and (b) the collision frequency between electron and neutral particles (solid line) and collision frequency between ion and neutral particles (dashed line).

horizontal magnetic field $H_{\perp}(n_x, n_y)/E_0$ on ground surface $z = 0$ and amplitude of electric field $E(n_x, n_y)/E_0$ at altitude $z = z_{\max}$ are presented in Figs. 2a,b. The field values are normalized by the value $E_0 = Z_0 J_0$. Polarization ellipse parameters ϕ , $E_{y'} = E_{x'} e^{-i\phi}$ and $\log|E_{y'}/E_{x'}|$ are presented in Figs. 2c,d. Positive values of phase ϕ correspond to right hand polarization, typical for whistler waves, and negative values of phase ϕ correspond to left hand polarization. Positive values of parameter 5 $\log|E_{y'}/E_{x'}|$ mean that the polarization ellipse is elongated predominantly along y axis and negative values of parameter $\log|E_{y'}/E_{x'}|$ mean that the polarization ellipse is elongated predominantly along x axis. Examples of altitude dependences of normalized electric and magnetic fields corresponding to different horizontal wave vectors are presented in Fig. 3. The level $z = z_s$ of source action is marked by dotted line. Figures 4 shows contour maps of fields created by horizontal currents with known space distribution. Figure 4a shows current density normalized by the value J_{\max} . Figure 4b shows electric field at the 10 altitude $z = z_{\max}$. Figure 4c shows horizontal magnetic field on ground surface $z = 0$. Both electric and magnetic fields are normalized by the value $Z_0 J_{\max}$. Figure 4d shows polarization parameter ϕ . The arrow shows the current direction.

5 Discussion

We use a full-wave approach to find the field of monochromatic whistler waves which are excited and propagating at night in the strongly inhomogeneous low ionosphere. A source current is assumed to be located in horizontal plane and to have 15 in this plane an arbitrary finite space distribution. At first, we consider a plane wave with the horizontal components of the refractive index \mathbf{n}_{\perp} generated by the current $J(\mathbf{r}_{\perp}) \sim e^{ik_0 \mathbf{n}_{\perp} \cdot \mathbf{r}_{\perp}}$. The set of wave equation in the layer $0 < z < z_{\max}$ for each \mathbf{n}_{\perp} - component is completed by boundary conditions assuming a perfect conductivity of ground surface and excluding wave energy coming on the upper boundary $z = z_{\max}$ from above. The method known as the two-point boundary-value problem for

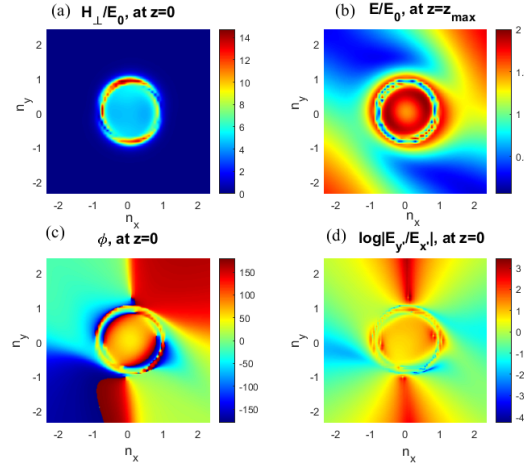


Figure 2. Fields in the $z = 0$ plane: (a) the horizontal magnetic field, (b) the electric field at the height $z = 125$ km, (c) the polarization ellipse parameters ϕ ($E_{y'} = E_{x'} e^{i\phi}$), and (d) $\log|E_{y'}/E_{x'}|$.

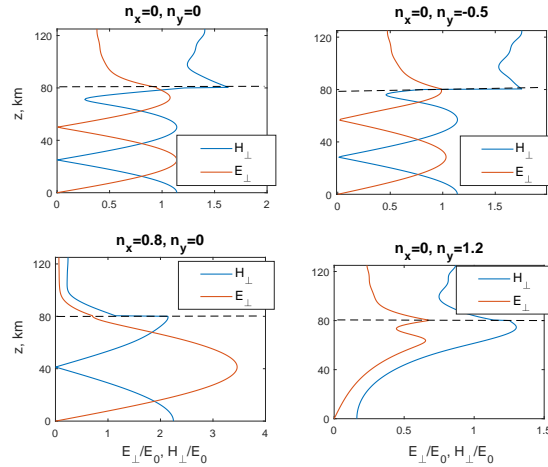


Figure 3. Altitude dependences of the amplitudes of horizontal electric and magnetic fields.

ordinary differential equations (Kierzenka and Shampine, 2001) is applied to find the solutions of wave equations above and below the source plane. Then we connect these solutions using source current distribution. When the dependencies of source current and wave field in n_{\perp} -space are finite functions with discretized values, the Fast Fourier Transform algorithm can be used for numerical calculations. Inverse Fast Fourier transform yields space dependence of the wave field.

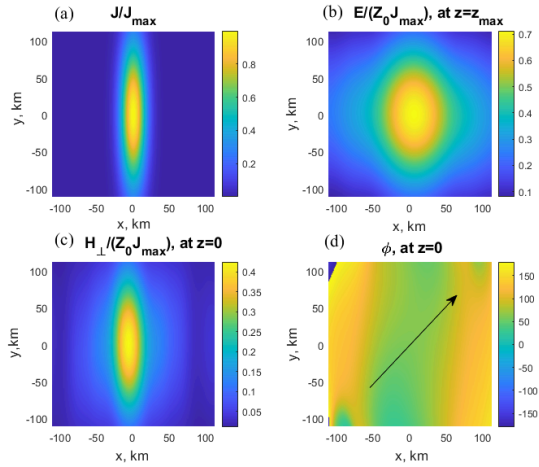


Figure 4. Source currents and fields space distributions: (a) space distributions of source currents, (b) the electric field at $z = 125$ km, (c) the horizontal magnetic field at $z = 0$, and (d) the polarization ellipse parameters ϕ , $E_{y'} = E_{x'} e^{-i\phi}$ at $z = 0$.

As an example, we calculate the fields created by varying at a frequency of 3 kHz and flowing at $z_s = 80$ km horizontal current, with coincided x and y components of current density $J_x = J_y$. We use a Gaussian distributions of source current density over x and y coordinates with characteristic horizontal sizes $L_x = 12$ km, $L_y = 70$ km. We mention that the model of a plane source current can also be effective in a more general case of current layer with small thickness $\Delta z \ll \lambda_z \sim 60$ km.

5 The ground-based horizontal magnetic field and the electric field at 125 km are calculated both in Fourier (n_x , n_y) and coordinate (x , y) spaces. Since a wave can achieve the ground surface in penetrating mode in case $n_{\perp} \leq 1$. The magnetic field $H_{\perp}(\mathbf{n}_{\perp}, z = 0)$ is noticeably non-zero for Fourier components with $n_{\perp} < 1$ and is practically equal to zero for Fourier components with $n_{\perp} \gg 1$. Waves with $n_{\perp} < 1$ are right hand polarized (see Fig. 2c), which is typical for whistlers. However, if the horizontal component of the refractive index has an order of unit, then the magnetic field $H_{\perp}(\mathbf{n}_{\perp}, z = 0)$ can increase 10 two or three times (see Fig. 2a). The polarization parameter ϕ of such components can be negative similar to the left hand polarized waves (see Fig. 2c). We mention that if the horizontal size of radiating currents is small enough $L \leq 1/k_0 \sim 15$ km (for wave with frequency 3 kHz) then Fourier components with $n_{\perp} \sim 1$ can make a noticeable contribution into the whole field and change the character of polarization.

15 The magnetic field $H_{\perp}(\mathbf{r}_{\perp}, z = 0)$ is predominantly localized under the source (Fig. 4c). The electric field at 125 km occupies a spot of several times larger size (Fig. 4b). The polarization parameter ϕ at $z = 0$ is positive almost everywhere, but becomes negative at large distances from the source across the current direction (Fig. 4d). We mention that the used in our calculation current distributions can be similar to electrojet currents modulated in D-region by the HAARP HF heating facility (Keskinen and Rowland, 2006; Payne et al., 2007). For example, according to data collected during an experimental campaign run in April 2003 and results of numerical simulations (Payne et al., 2007; Lehtinen and Inan, 2008), the maximum change in

modulated conductivity occupies approximately 10 km over the height and occurs at altitude ~ 80 km. Pedersen and Hall conductivities approximately coincide so if ambient electrojet field is directed along x axis, then $j_x \approx j_y$. The maximum surface density of modulated currents has an order $J_{\max} \sim 10^{-6} \div 10^{-5} \text{ Am}^{-1}$. Using in our calculations the magnitude of current density $J_{\max} \sim 5 \cdot 10^{-6} \text{ Am}^{-1}$ yields the total power of the source $\sim 36 \text{ W}$, the ground-based horizontal magnetic field under the source $B_{\perp} \sim 1 \text{ pT}$ and the electric field at the altitude of 125 km above the source $E \sim 400 \mu \text{Vm}^{-1}$. The magnitude of the magnetic field is similar to the field measured at VLF sites in the immediate vicinity of the HAARP heating facility (Payne et al., 2007) and calculated by Lehtinen and Inan (2008). The maximum vertical energy flux (Poynting vector) at the altitude of 125 km is $\sim 3,2 \text{nWm}^{-1}$ and total power is $\sim 17 \text{ W}$. The percentages of source energy supplied by the Earth-ionosphere waveguide and carried upward ionosphere depends on altitude profile of ionosphere plasma. If low boundary of ionosphere is sharp enough then sufficient part of the source energy is supplied to the Earth-ionosphere waveguide. In a case of smooth ionosphere low boundary sufficient part of the source energy is carried upward. By used for calculation altitude profile of plasma density about half of the source energy is carried upward, approximately twenty percent of the energy is supplied to the Earth-ionosphere waveguide and approximately thirty percent of the energy is absorbed.

6 Conclusions

We find a field of monochromatic whistler waves which are excited and propagating in the low nighttime ionosphere. Using a MatLab boundary-value problem solver enables to find numerically stable solutions of full set of the wave equations applying to conditions of inhomogeneous ionosphere at altitudes below 125 km. Above this altitude the ionosphere plasma is slightly inhomogeneous, hence approximate methods are suitable. As example, this calculation technique is applied to the problem of ELF/VLF waves radiation from modulated HF-heated electrojet currents. At first we consider a plane wave with known horizontal component of the refractive index, find a wave field and analyze a character of wave polarization on the ground surface. Then we use inverse Fast Fourier transform to find a total field, get the dependencies of wave field at 0 km and 125 km, analyze the type of wave polarization on the ground surface and estimate absorbed, supplied by the earth-ionosphere waveguide and carried upward parts of source energy. The obtained values are in a good agreement with ground and satellite observations and known calculation results. Using model of plane horizontal source currents can be generalized for the arbitrary altitude source distribution.

Data availability. The paper is theoretical and no new experimental data are used. The data are taken from International Reference Ionosphere model (Bilitza and Reinisch, 2007) (https://ccmc.gsfc.nasa.gov/modelweb/models/iri2016_vitmo.php). All figures are obtained from numerical calculation in MATLAB codes.

Author contributions. VM produced the calculations, analyzed results, and wrote the paper. PB proposed the problem, discussed results, and wrote the paper.

Competing interests. The authors declare that they have no conflict of interest.

Acknowledgements. The work (Sections 2-4) is supported by RFBR grant No. 20-02-00206A. The work of P.A. Bespalov (Sections 1, 5, and 6) is supported by RSF grant No. 20-12-00268. The numerical calculations were performed as part of the State Assignment of the Institute of Applied Physics RAS, project No.0035-2019-0002.

References

Bespalov, P. and Mizonova, V.: Propagation of a whistler wave incident from above on the lower nighttime ionosphere, *Ann. Geophys.*, 35, 671-675, <http://dx.doi.org/10.5194/angeo-35-671-2017>, 2017.

Bespalov, P.A., Mizonova V.G., and Savina, O.N.: Reflection from and transmission through the ionosphere of VLF electromagnetic waves incident from the mid-latitude magnetosphere, *J. Atmos. Sol.-Terr. Phys.*, 175, 40-48, <https://doi.org/10.1016/j.jastp.2018.04.018>, 2018.

Bilitza, D., and Reinisch, B.: International reference ionosphere: improvements and new parameters, *J. Adv. Space Res.*, 42, 599 - 609, <http://dx.doi.org/10.1029/2007SW000359>, 2007.

Bossy, L.: Wave propagation in stratified anisotropic media, *J. Geophys.*, 46, 1-14, 1979.

Budden, K.G.: The propagation of radio waves: the theory of radio waves of low power in the ionosphere and magnetosphere, Cambridge Univ. Press, Cambridge, 1985.

Cooley, W. and Tukey, J.W.I.: An algorithm for the machine calculation of complex Fourier series, *Math. Comp.*, 19, 297-301, <https://doi.org/10.1090/S0025-5718-1965-0178586-1>, 1965.

Gurevich, A.V. and Shvarcburg, A.B.: Nonlinear theory of radio wave propagation in the ionosphere, Nauka, Moscow, 1973 [in Russian].

Keskinen, M.J., and Rowland, H.L.: Magnetospheric effects from man-made ELF/VLF modulation of the auroral electrojet, *Radio Sci.*, 41, 15 RS1006, <https://doi:10.1029/2005RS003274>, 2006.

Kierzenka, J., and Shampine, L.F.: A BVP Solver based on Residual Control and the MATLAB PSE , *ACM TOMS.*, 27, 3, 299-316, 2001.

Lehtinen, N.G., and Inan, U.S.: Radiation of ELF/VLF waves by harmonically varying currents into a stratified ionosphere with application to radiation by a modulated electrojet, *J. Geophys. Res.*, 113, A06301. <http://dx.doi.org/10.1029/2007JA012911>, 2008.

Mizonova, V.G.: Matrix Algorithm of Approximate Solution of Wave Equations in Inhomogeneous Magnetoactive Plasma, *Plasma Phys. Rep.*, 45, 8, 777-785, <https://doi:10.1134/S1063780X190700802019>, 2019.

Nagano, I., Miyamura, K., Yagitani, S., Kimura, I., Okada, T., Hashimoto, K., and Wong, A.Y.: Full wave calculation method of VLF wave radiated from a dipole antenna in the ionosphere - analysis of joint experiment by HIPAS and Akebono satellite, *Electr. Commun. Jpn. Commun.*, 77, 59-71, <http://dx.doi.org/10.1002/ecja.4410771106>, 1994.

Nygren, T.: A method of full wave analysis with improved stability, *Planet. Space Sci.*, 30(4), 427-430, [http://dx.doi.org/10.1016/0032-0633\(82\)90048-4](http://dx.doi.org/10.1016/0032-0633(82)90048-4), 1982.

Payne, J.A., Inan, U.S., Foust, F.R., Chevalier, T.W., and Bell, T.F.: HF modulated ionospheric currents, *Geophys. Res. Lett.*, 34, L23101, <http://doi:10.1029/2007GL031724>, 2007.

Pitteway, M.L.V.: The numerical calculation of wave-fields, reflection coefficients and polarizations for long radio waves in the lower ionosphere, *I. Phil. Trans. R. Soc. London, Ser. A*, 257(1079), 219-241, 1965.

Shalashov, A. G. and Gospodchikov, E. D.: Impedance technique for modeling electromagnetic wave propagation in anisotropic and gyroscopic media, *Physics-Uspekhi*, 54, 145- 165, <https://doi.org/10.3367/UFNe.0181.201102c.0151>, 2011.

Wait, J.R.: Electromagnetic waves in stratified media, 2nd ed., Pergamon, New York, 1970.

Yagitani, S., Nagano, I., Miyamura, K., and Kimura, I.: Full wave calculation of ELF/VLF propagation from a dipole source located in the lower ionosphere, *Radio Sci.*, 29, 39-54, <https://doi:10.1029/93RS01728>, 1994.